Volume 1 | Number 1 | Jan 2013 | Pages 1–100

Organic &
Biomolecular
Chemistry

www.rsc.org/obc

ROYAL SOCIETY
OF CHEMISTRY

This is an *Accepted Manuscript*, which has been through the
Royal Society of Chemistry peer review process and has been
accepted for publication.

Accepted Manuscripts are published online shortly after
acceptance, before technical editing, formatting and proof reading.
Using this free service, authors can make their results available
to the community, in citable form, before we publish the edited
article. We will replace this *Accepted Manuscript* with the edited
and formatted *Advance Article* as soon as it is available.

You can find more information about *Accepted Manuscripts* in the
Information for Authors.

Please note that technical editing may introduce minor changes
to the text and/or graphics, which may alter content. The journal's
standard **Terms & Conditions** and the **Ethical guidelines** still
apply. In no event shall the Royal Society of Chemistry be held
responsible for any errors or omissions in this *Accepted Manuscript*
or any consequences arising from the use of any information it
contains.

www.rsc.org/obc

ROYAL SOCIETY
OF CHEMISTRY

Journal Name

ARTICLE

A Mechanistic Study on the Inhibition of α-Chymotrypsin by a Macrocyclic Peptidomimetic Aldehyde

X. Zhang,[ab] J.B. Bruning,[c] J.H. George[b] and A. D. Abell[ab†]

Here we describe an NMR and X-ray crystallography-based characterisation of the mechanism by which a new class of macrocyclic peptidomimetic aldehyde inhibits α-chymotrypsin. In particular, a ^{13}C-labelled analogue of the inhibitor was prepared and used in NMR experiments to confirm formation of a hemiacetal intermediate on binding with α-chymotrypsin. Analysis of an X–ray crystallographic structure in complex with α-chymotrypsin reveals that the backbone adopts a stable β-strand conformation as per its design. Binding is further stabilised by interaction with the oxanion hole near the S_1 subsite and multiple hydrogen bonds.

Introduction

Proteases almost universally bind their substrates and inhibitors in a conformation whereby the peptide or peptide-like backbone adopts a β-strand, a geometry that complements key binding sites in the protease active site.[1-6] An important approach to inhibitors is to introduce a carefully designed macrocyclic constraint into the structure to pre-organise its backbone into an extended conformation, thereby reducing entropy loss associated with ligand-receptor binding, while also enhancing biostability (see **1-5**, Fig. 1).[7-21] This typically involves chemically linking either the P_1 and P_3 or the P_1' and P_3' residues of the inhibitor backbone. For example see compounds **3**,[22] **4**[23, 24] and **5**[25] (Fig. 1), which target m-calpain, the 20S proteasome and HIV-1 protease respectively.

We recently reported a new generation of macrocyclic protease inhibitor that has a backbone amino acid and an associated peptide bond replaced with a planar aromatic pyrrole, e.g. see macrocycles **6** and **7** (Fig. 2).[26] As a result the ligand has significantly reduced peptide character, while retaining the before mentioned backbone β-strand geometry required for active site binding. The macrocycle of these structures links the P_2 amino acid and *N*-terminus to leave the P_1 position free to incorporate appropriate functionality (e.g. amino aldehyde, amino dicarbonyl, heterocycle, isosteres, and other moieties)[27-38] to provide an opportunity to target a given protease. Macrocycle **6** with its aliphatic macrocycle, isopropyl

group at P_1 to mimic leucine, and a *C*-terminal aldehyde, exhibits pico-molar activity against cathepsins S and L.[26] The incorporation of aryl groups into the macrocycle as in **7** gives rise to a potent and selective inhibitor of α-chymotrypsin, with a K_i of 33 nM.
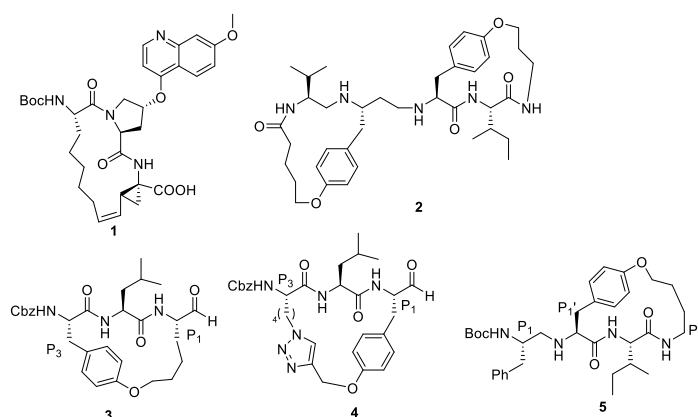
Fig. 1 Examples of macrocyclic protease inhibitors. The amino acid residues are defined according to nomenclature developed by Schechter and Berger.[39]

7: R = CHO
8: R = C[13]HO
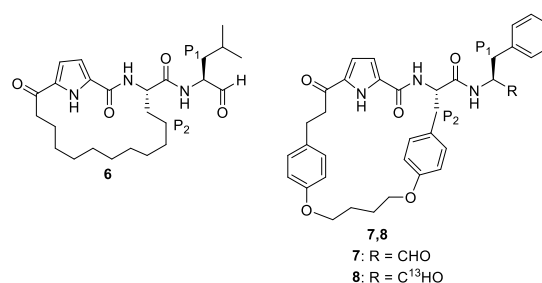
Fig. 2 New pyrrole-containing macrocyclic protease inhibitors linked from P_2 side chain to N-terminus.

a. *ARC Centre of Excellence for Nanoscale BioPhotonics (CNBP), Institute for Photonics and Advanced Sensing, Department of Chemistry, The University of Adelaide, Adelaide, SA 5005, Australia.*
b. *Department of Chemistry, The University of Adelaide, Adelaide, SA 5005, Australia.*
c. *School of Biological Sciences, The University of Adelaide, Adelaide, SA 5005, Australia.*
† Corresponding author, email: andrew.abell@adelaide.edu.au

Here we report a combination of NMR and X-ray crystallographic studies to characterize the mode of binding and mechanism of inhibition of this new class of macrocyclic inhibitor. The macrocycle **7** was chosen for this study for ease of solving an α-chymotrypsin-ligand X-ray structure[26] and to allow the incorporation of a ^{13}C label in the formyl group as shown (compound **8**, Fig. 2) for NMR studies as reported here.

Results and Discussion

Synthesis of macrocycles 7 and 8. The conditions used in the synthesis of **7** and **8** were optimised from our earlier report.[26] Yb(III)(OTf)$_3$-catalysed Friedel-Crafts acylation of pyrrole derivative **9** and acid chloride **10** was first attempted using literature conditions[26] and this gave the key dipeptide-mimic **11** in a low yield of 16%. Several alternative conditions for the preparation of **11** were thus investigated, with the optimum temperature and reaction time proving to be 45 °C and 48 h, respectively. A large-multi gram scale reaction under these conditions gave the desired product **11** in an improved yield of 58%. Hydrolysis of the ethyl ester of **11** with KOH gave the corresponding carboxylic acid, which was directly coupled with O-allyl-tyrosine methyl ester in the presence of HATU, HOBt and DIPEA to give diene **12** in 78% yield over two steps. Treatment of **12** with two portions of Grubbs second-generation catalyst (10%/portion) in highly dilute conditions (1.3 mM) gave the desired unsaturated macrocycle. Hydrogenation of the olefin was first attempted on a small scale (100 mg) on treatment of 10% (mol %) Pd/C for 18 h and this gave the saturated macrocycle **13** in 24% yield. A repeat using an increased loading (33%, mol %) of Pd/C and a shorter reaction time of 3 h gave an improved yield of 76% over two steps. The methyl ester of **13** was then hydrolysed with NaOH to give the free acid **14**, which was coupled to *L*-phenylalaninol in the presence of HATU, HOBt and DIPEA to give macrocyclic alcohol **15** in 48% yield. The primary alcohol was subsequently oxidized with Dess-Martin periodinane to give the desired macrocyclic aldehyde **7**. The ^{13}C-labelled analogue **8** was similarly prepared by coupling ^{13}C phenylalaninol **18** with the macrocyclic acid **14**, with a final oxidation of the primary alcohol to the aldehyde, see Scheme 2. The alcohol **18** was prepared from commercially available *L*-phenylalanine-1-[13]C **16** as shown in Scheme 2. Specifically, the free amine of **17** was reacted with Boc-anhydride and the carboxylic acid was reduced with LiAlH$_4$ to give **17** in quantitative yield. The Boc group was subsequently removed on treatment of TFA, in DCM, to give **18** in 98% yield over three steps.
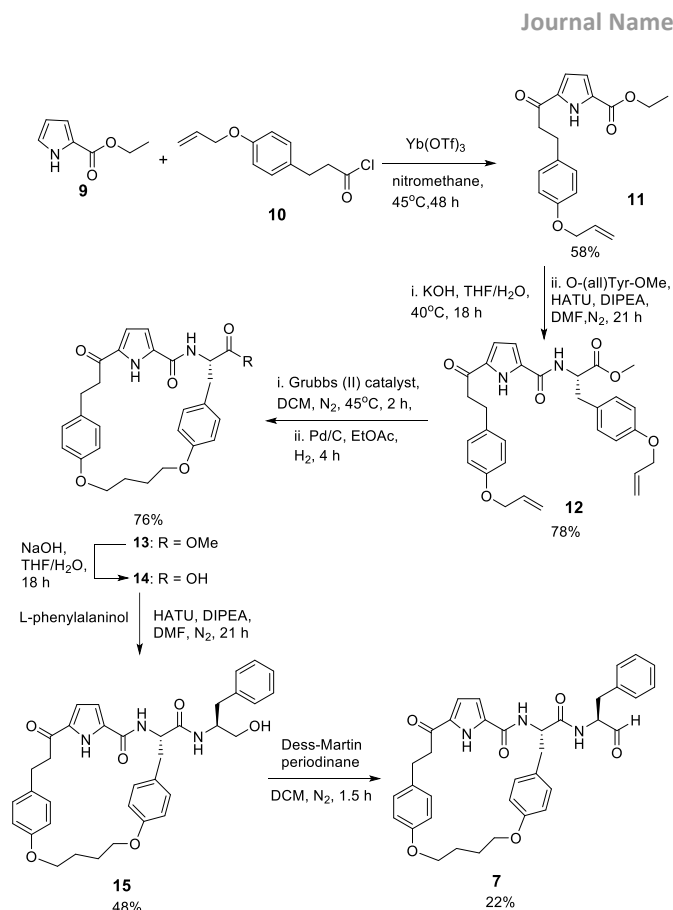

Scheme 1 Synthesis of compound **7**.
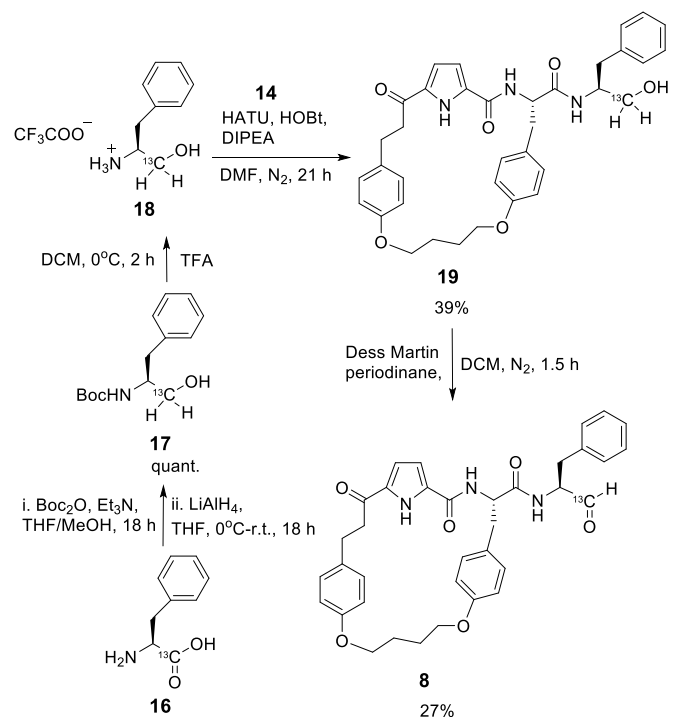

Scheme 2 Synthesis of labelled aldehyde **8**.

¹³C NMR study of α-chymotrypsin-8 complex. A ¹³C NMR spectrum of the ¹³C-labelled aldehyde **8** in CDCl₃ revealed a 100-fold enhancement in the intensity of the aldehyde resonance at 199.6 ppm relative to the unlabelled aldehyde **7**, making it an ideal tag for enzyme/inhibitor studies. Some initial experiments were carried out to optimise the solvent system for the enzyme inhibition studies. Unfortunately ¹³C-labelled **8** was not freely soluble in 7.5% DMSO-d_6 in D₂O, a solvent system used in other NMR study involving α-chymotrypsin.[40] Solubility was not visibly improved on stirring this suspension for 1 h at room temperature and as such it was not possible to determine the concentration of inhibitor **8** under these conditions (Figure S3, supporting information). The activity of α-chymotrypsin was thus assayed *in vitro* using a fluorogenic substrate alanine-alanine-phenylalanine-AMC (AAF-AMC) and increasing concentrations of DMSO in order to determine the enzyme's tolerance for this solvent. α-Chymotrypsin activity is directly proportional to the rate of fluorescence increase in this assay, which is equivalent to the slope of the linear plot shown in Fig. 3. A positive control (Fig. 3, blue) containing α-chymotrypsin and AAF-AMC in 2.5% DMSO in H₂O gave a gradient of 139.7. Increasing the DMSO content to 10% (Fig. 3, green) and 20% (Fig. 3, red) gave gradients of 119.1 and 96.5 respectively. This indicates that α-chymotrypsin in 20% DMSO in H₂O retained 69% activity compared to the positive control. It was anticipated that this level of activity would be sufficient for the proposed ¹³C NMR experiments using labelled aldehyde **8** and the study was continued on this premise.
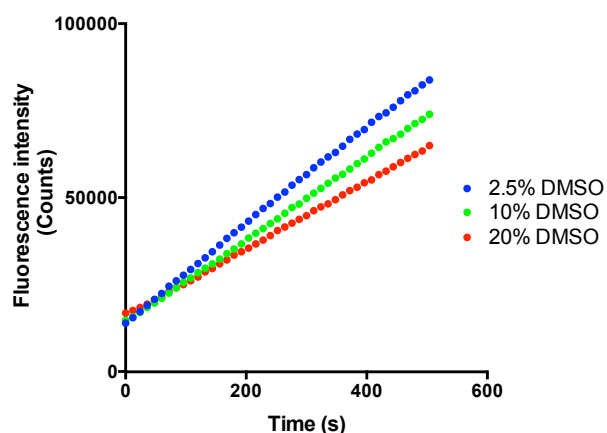
Fig. 3 α-Chymotrypsin activity in water containing 2.5% (blue), 10% (green) or 20% (red) DMSO.

Six solutions of **8** in DMSO (concentrations of 0.2, 0.3, 0.4, 1, 1.5 and 2 mM) were prepared and 20 μL of each solution was subjected to reverse phase HPLC with detection at λ = 280 nm. The absolute integral of the peak at 18.1 min, corresponding to **8**, was calculated for each injection and these results were plotted against the amount of **8** injected to construct a standard curve for determining unknown concentrations of **8** for a given amount of DMSO in H₂O (Fig. 4). Next, a saturated solution of **8** was prepared by adding an excess to 20% DMSO in H₂O with stirring at room temperature for 1 h. This suspension was centrifuged and filtered to give a

homogeneous solution and 20 μL of this was analysed as before by HPLC. An analysis using the standard curve indicated a concentration of 2.6 mM, which represents the saturation concentration of **8** in 20% DMSO/H₂O under these conditions. This value is comparable with the concentration of an unrelated inhibitor used in a related NMR experiment as reported previously.[40]
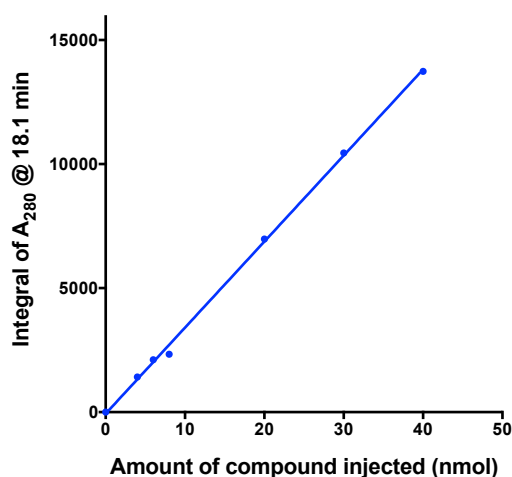

Fig. 4 A graph of peak integral versus amount of compound **8** injected. A linear line was fitted to the graph with GraphPad Prism 6.

¹³C NMR spectroscopy was then used to study the interaction of macrocyclic aldehyde **8** with α-chymotrypsin under these conditions. A ¹³C NMR spectrum of a sample of **8** (2.6 mM in 20% DMSO-d_6 in D₂O, see blue trace in Fig. 5) revealed a resonance of enhanced intensity at 200.5 ppm, corresponding to the *C*-terminal aldehyde of **8**, and a second resonance at 89.9 ppm. The chemical shift of this second resonance is consistent with a hemiacetal formed on reaction of the aldehyde with D₂O.[41] A ¹³C NMR spectrum of compound **8** (2.6 mM in the same solvent system) with added α-chymotrypsin (2.6 mM), is shown in red in Fig. 5. This reveals a single new resonance at 92.3 ppm, which is consistent with a hemiacetal formed on reaction with active site Ser₁₉₅ (Scheme 3). The initial resonances at 200.5 ppm and 89.9 ppm were not observed as expected for a highly efficient reaction of the aldehyde of **8** with the active-site serine of α-chymotrypsin. This is consistent with simple acyclic peptidic aldehyde inhibitors, which are also reported to form a hemiacetal on the reaction with the active site serine of α-chymotrypsin.[41-43]

(a)

(b)
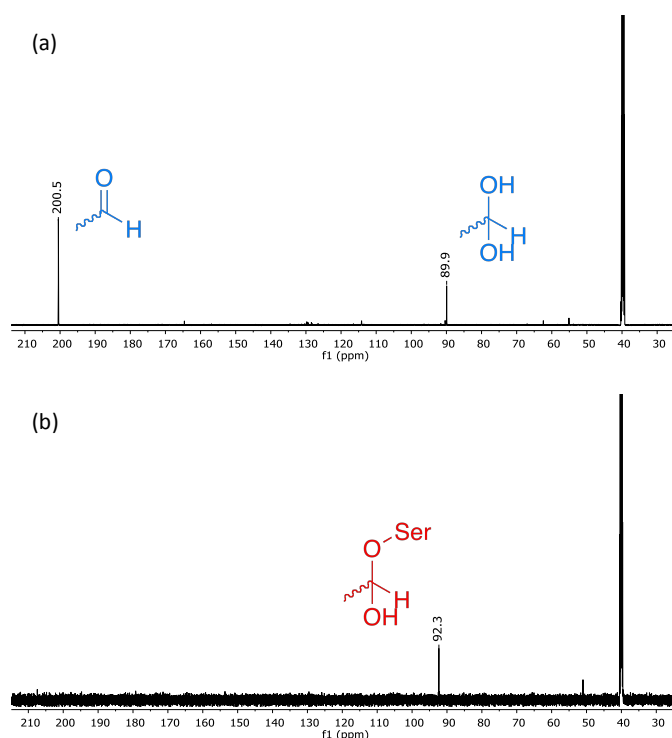
Fig. 5 (a) ^{13}C NMR spectrum of compound **8** in 20% DMSO-d_6 in D_2O (2.6 mM) without added enzyme; (b) ^{13}C NMR spectrum of α-chymotrypsin (2.6 mM) and **8** (2.6 mM) in 20% DMSO-d_6 in D_2O.
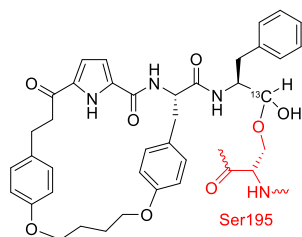

Scheme 3. *C*-terminal aldehyde of **8** reacts with Ser195 of α-chymotrypsin (red) to form a hemiacetal.

A single crystal structure of the α-chymotrypsin-**7** complex,[26] solved to a resolution of 2.2Å, was analysed in detail to reveal the nature of the covalent attachment and the nature of other non-covalent interactions. Overall, α-chymotrypsin crystallised in a tetrameric form in the asymmetric unit with each monomer bound by one molecule of compound **7**. The inhibitor binds within the active site of α-chymotrypsin as shown in Fig. 6a. The P_1 phenylalanine of **7** binds with the S_1 subsite defined by amino acids Ser189-Met192, Ser214-Gly216 and Trp224-Tyr228 (Fig. 7, b). This orients the *C*-terminal aldehyde to less than 1.5 Å away from the catalytic Ser195 of α-chymotrypsin, which is a feasible distance for the formation of a covalent bond as identified above. In addition, the electron density map (Fig. 7) shows continuous electron density between **7** and Ser195. This also indicates the existence of a covalent bond between the aldehyde carbon of **7** and the side-chain hydroxyl group of Ser195, which is consistent with the observations of the ^{13}C NMR experiments reported above. The P_2 aryl group, as a part of

the macrocycle, binds with the S_2 pocket of α-chymotrypsin. The binding is stabilised by a π-π interaction with His$_{57}$, a member of the catalytic triad. As per our design, the backbone of the bound inhibitor adopts an extended geometry similar to a β-strand (Fig. 8, a), with dihedral angles φ = 147°, ψ = -88°, and ϖ = 178° (Fig. 8, b) respectively.

(a)

(b)
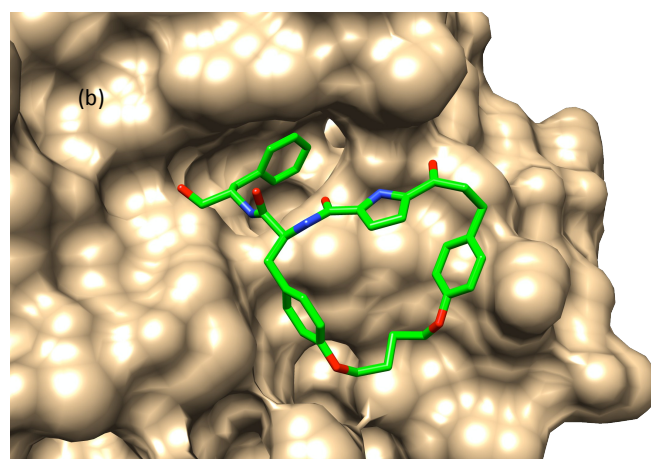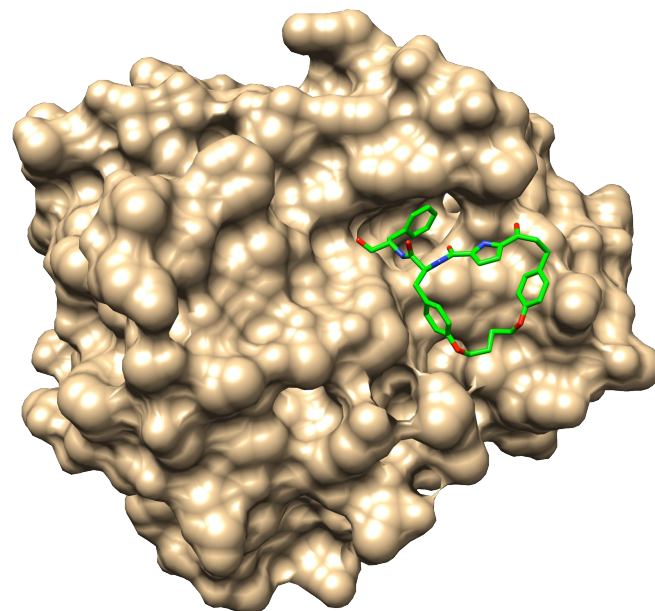
Fig. 6 (a) An X-ray crystal structure of an α-chymotrypsin monomer bound by compound **7** in its active site; (b) the expansion to the active site region of α-chymotrypsin. The enzyme is displayed as surfaces in light brown and the inhibitor is displayed as sticks in green (PDB: 4Q2K).
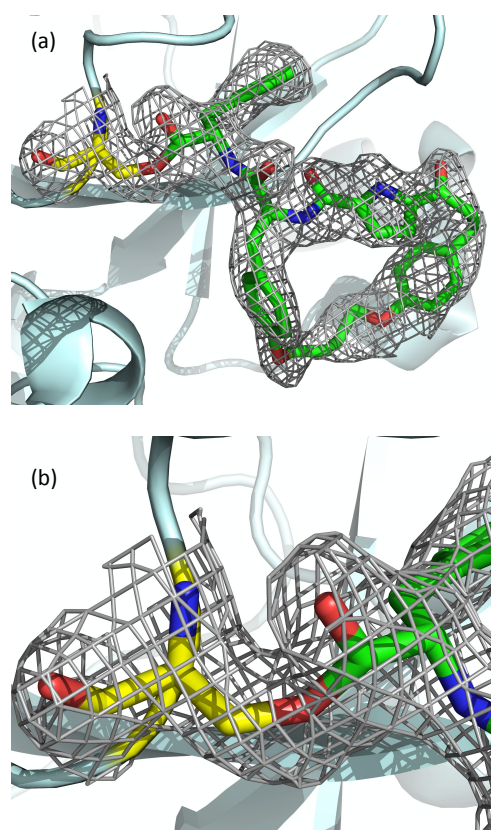
Fig. 7 (PDB:4Q2K). (a) $2F_o$-F_c kicked electron density map (in grey) of compound **7** contoured at 1σ, the inhibitor is displayed in sticks coloured by element and the enzyme is displayed in ribbons; (b) an expansion to the region of Ser195 and the warhead.
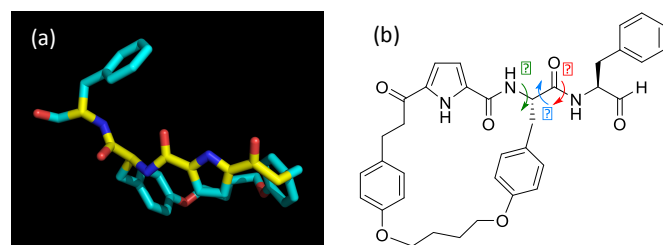

Fig. 8 (a) X-ray crystallographic structure of compound **7** bound to α-chymotrypsin (backbone highlighted in yellow) (PDB:4Q2K); (b) Chemical structure of **7** showing the measured dihedral angles.

Compound **7** forms a number of hydrogen bonding interactions with the active site of α-chymotrypsin as illustrated in Fig. 9. For example, the 'aldehyde oxygen' of **7** interacts directly with the backbone amine of Ser195 and Gly193 that form the oxyanion hole. The oxyanion hole stabilises the negatively charged oxygen atom of the hemiacetal intermediate (Fig. 10, green), which, in this case, is formed upon reaction with the aldehyde of compound **7**. This would be expected to enhance binding affinity of inhibitor **7.** Many of the hydrogen bonding interactions are mediated by water molecules. Two of these molecules, denoted as Hoh260 and Hoh491 in Fig. 8, have particular importance in mediating hydrogen bonding interactions. Hoh260 interacts with Thr222 of the enzyme,

C33 of the inhibitor and two other water molecules, while Hoh491 interacts with Gly216 and Ser217 of the enzyme, pyrrole NH and O30 of **7**, and Hoh430. These hydrogen bonding interactions play crucial roles in the stabilisation of the α-chymotrypsin-**7** complex. The binding affinity of the inhibitor is further enhanced by hydrophobic and ionic interactions with other critical active site residues, including His57 and Asp102 of the catalytic triad. Upon binding, the macrocycle linking P_2 and P_4 side chains of **7** lies exactly parallel to Trp215, which potentially facilitates π-π interactions with the enzyme.
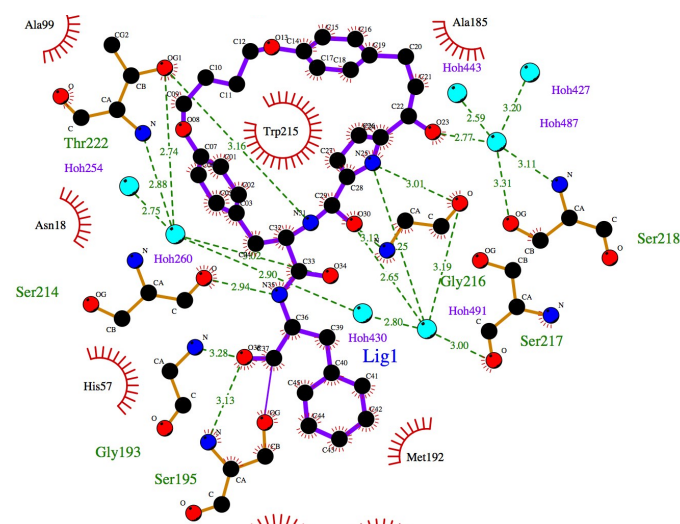
Fig. 9 A ligplot showing non-covalent interactions of compound **7** and α-chymotrypsin. The inhibitor and amino acids of α-chymotrypsin involved in hydrogen bonding interactions are displayed in a ball-and-stick representation. The amino acids involved in other non-covalent interactions are displayed as arcs.
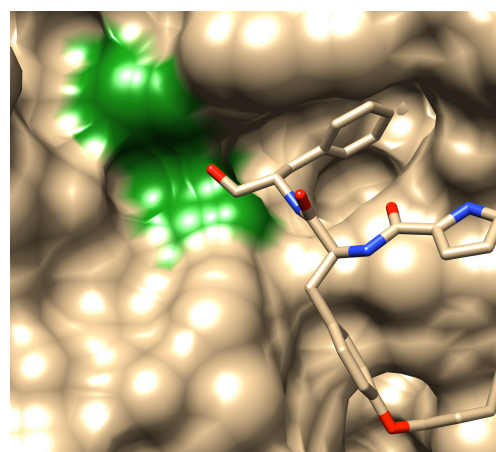
Fig. 10 The oxyanion hole (green) of α-chymotrypsin stabilises the active-site binding of compound **7**. The enzyme is displayed as a surface representation and the inhibitor is displayed as sticks coloured by element. (PDB:4Q2k).

The P_2-P_4 backbone of the enzyme-bound inhibitor **7** superimposes nicely with the backbone of several natural peptide-based inhibitors, including ecotin (pink, Fig. 10a), guamerin (green, Fig.

11a) and PMP-C (blue, Fig. 11a). These structures are known to bind α-chymotrypsin in an extended β-strand conformation.[26, 44-46] The pyrrole group of inhibitor **7** clearly helps to define its backbone geometry while occupying the space between the S_3 and S_4 subsites of the enzyme. The P_1 phenyl group also overlays perfectly with the P_1 side chains of PMP-C, guamerin and ecotin, which poses the *C*-terminal aldehyde in close proximity to Ser195 to allow covalent reaction. A previous study was similarly conducted with co-crystallisation of an aldehyde inhibitor Ac-LF-CHO in α-chymotrypsin.[42] An overlay of the two crystal structures (Fig. 11b) shows that the P_1 residues of **7** and Ac-LF-CHO superimpose perfectly, with both aldehyde groups binding in the oxyanion hole. The P_2 side chain of inhibitor **7** partially overlays with the leucine side chain of Ac-LF-CHO. This confirms that the macrocycle does not interrupt binding with the S_2 subsite.
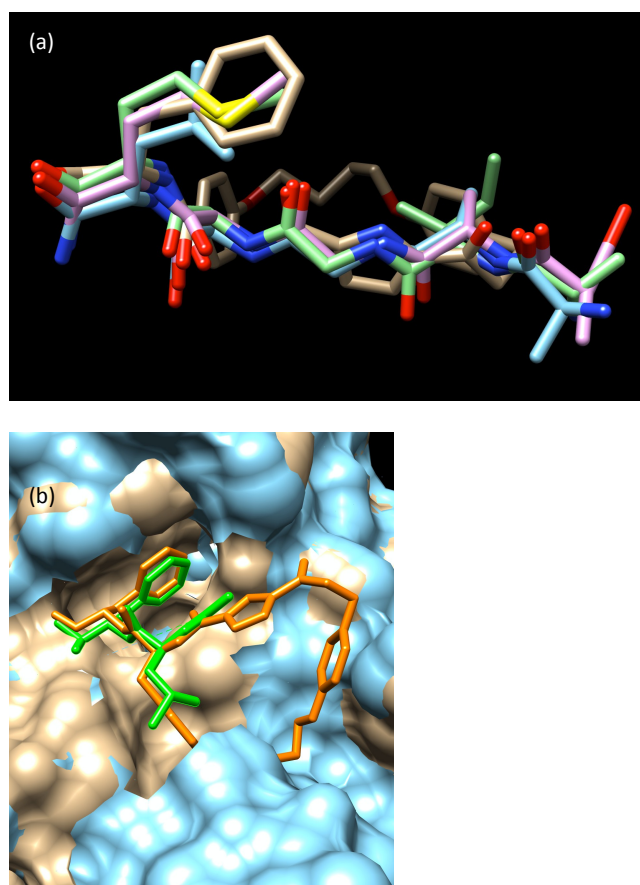
Fig. 11 The superimposition of crystal structures of a) enzyme-bound **7** (backbone in beige), natural protease inhibitors ecotin (backbone in pink, PDB: 2Y6T),[44] guamerin (backbone in green, PDB: 3BG4)[45] and PMP-C (backbone in blue, PDB: 1GL1);[46] and b) compound **7** (in orange) and Ac-LF-CHO (in green, PDB: 1GGD)[42] in the active site of α-chymotrypsin.

Conclusions

In summary, the binding of a peptidomimetic protease inhibitor **7/8** with α-chymotrypsin was characterized by NMR and X-ray crystallography. The key features of this inhibitor include a pyrrole

moiety replacing the P_3 amino acid and a macrocycle linking the P_2 side chain and *N*-terminus. These features work in synergy to constrain the inhibitor backbone into an extended β-strand geometry, while also potentially increasing the resistance to random proteolysis. The P_2 to *N*-terminus cyclisation also allows easy modification of the P_1 residue, which is critical for providing selectivity and potency to this new class of protease inhibitor. The incorporation of a ^{13}C-label on the terminal aldehyde of the inhibitor amplified the signal intensity in carbon NMR by 100-fold, making it easily distinguishable from other carbon signals of the inhibitor and enzyme. The ^{13}C NMR spectrum of the inhibitor-enzyme complex shows efficient formation of a new intermediate with chemical shift corresponding to a hemiacetal formed on reaction of the aldehyde with serine hydroxyl. A crystal structure of the enzyme-inhibitor complex demonstrates that the P_1 phenyl group binds tightly with the S_1 subsite, thus promoting the reaction between the aldehyde and active site serine to form a hemiacetal intermediate. The backbone of the inhibitor was shown to adopt a β-strand-mimicking geometry introduced by macrocyclisation, which is consistent with our design.

Experimental Section

I. Chemical Syntheses

General Information. Unless otherwise indicated, all starting materials, enzymes, chemicals and anhydrous solvents were purchased from Sigma Aldrich (NSW, Australia) and were used without further purification. Compounds **7**, **9**, **10**, **12**, **14**, **15** and *O*-(allyl)tyrosine methyl ester were prepared as previously described.[26] ^{1}H and ^{13}C NMR spectra were recorded on a Varian 500 MHz and a Varian Inova 600 MHz instruments in the indicated solvents. Chemical shifts are reported in ppm (δ). Signals are reported as s (singlet), br s (broad singlet), d (doublet), dd (doublet of doublets), t (triplet) or m (multiplet). High resolution mass spectra were collected using an LTQ Orbitrap XL ETD using flow injection, with a flow rate of 5 μL/min. Where indicated compounds were analyzed and purified by reverse phase HPLC, using an HP 1100 LC system equipped with a Phenomenex C-18 column (250 × 4.6 mm) for analytical traces and a Gilson GX-Prep HPLC system equipped with a Phenomenex C18 column (250 × 21.2 mm). H_2O/TFA (100/0.1 by v/v, A) and ACN/TFA (100/0.08 by v/v, B) solutions were used as aqueous and organic buffers. All graphs were generated using GraphPad Prism 6 software. Protein crystallography was performed as reported previously.[26] Crystal structures were visualised by Pymol 1.3, Coot 0.7 and UCSF Chimera 1.9. Structural superimposition was obtained from MatchMaker in UCSF Chimera 1.9.

^{13}C-labelled macrocyclic aldehyde (8). Compound **14** (38 mg, 0.06 mmol) was dissolved in anhydrous DCM (9 mL). Dess-Martin periodinane (76 mg, 0.18 mmol) was added under N_2 at room temperature. The mixture was stirred under N_2 at room temperature for 1.5 h. The reaction was quenched by slow addition of $Na_2S_2O_5$ (35 mg) in sat. $NaHCO_3$ (6 mL). The aqueous phase was extracted with DCM (2 × 10 mL). The organic phases were combined and dried over $MgSO_4$. The solvent was removed *in vacuo* and the resultant crude product was purified with RP-HPLC to give compound **8** as a pale yellow oil (10 mg, 27%). ^{1}H NMR (500 MHz,

CDCl$_3$) δ 9.90 (br s, 1H), 9.68 (d, J = 179.8 Hz, 1H), 7.20 – 7.07 (m, 5H), 7.00 (d, J = 8.5 Hz, 2H), 6.91 (d, J = 8.5 Hz, 2H), 6.76 (d, J = 8.5 Hz, 2H), 6.63 (d, J = 8.5 Hz, 2H), 6.16 – 6.09 (m, 2H), 6.05 – 6.00 (m, 1H), 4.81 – 4.67 (m, 2H), 4.01 – 3.76 (m, 4H), 3.30 – 2.87 (m, 7H), 1.94 (br s, 4H). ^{13}C NMR (151 MHz, CDCl$_3$) selected data shows ^{13}C-enriched aldehyde at δ 198.5. Analytical RP-HPLC: t_R = 18.1 min (A/B 100 : 0 to 0 : 100 in 20 min, λ = 220 nm). HRMS (ESI) found [M]$^+$ 608.2725, C$_{35}$^{13}CH$_{37}$N$_3$O$_6$$^+$ requires 608.2716.

Ethyl 5-(3-(4-(allyloxy)phenyl)propanoyl)-1H-pyrrole-2-carboxylate (11). To a solution of compound **9**[26] (2.3 g, 10.00 mmol) in nitromethane (27 mL) was added **10**[26] (700 mg, 5.00 mmol) and Yb(OTf)$_3$ (310 mg, 0.50 mmol). The dark red mixture was stirred at 45 °C for 48 h. The reaction was quenched by addition of sat. NaHCO$_3$ (250 mL). The mixture was extracted with Et$_2$O (3 × 250 mL). The combined organic phase was washed with sat. NaHCO$_3$ (250 mL), H$_2$O (2 × 200 mL) and brine (250 mL) and dried over MgSO$_4$. The solvent was removed *in vacuo* and the resultant brown oil was purified by flash chromatography (Et$_2$O/hexane 2:3) to give compound **11** as a yellow solid (48 mg, 32%). ^{1}H NMR as previously reported.[26]

Macrocyclic ester (13). To a solution of compound **12**[26] (260 mg, 0.53 mmol) in anhydrous DCM (100 mL) was added Grubb's 2nd generation catalyst (45 mg, 0.06 mmol). The mixture was heated to 45 °C and stirred for 1 h under a nitrogen atmosphere after the addition of the first portion. An additional portion of Grubb's 2nd generation catalyst (45 mg, 0.06 mmol) was added and the solution was stirred for 18 h at 45 °C. The reaction was quenched by addition of activated charcoal and stirred at room temperature for 18 h. The solvent was removed *in vacuo* and the resultant crude product (295 mg) was dissolved in EtOAc (120 mL) under H$_2$. Pd/C (97 mg, 33% w/w) was added to the solution and the mixture was stirred at room temperature under H$_2$ for 3 h. The mixture was then filtered through celite and the solvent was removed *in vacuo.* The resultant crude product (293 mg) was purified by flash chromatography (petroleum ether:EtOAc 1:1) to give compound **13** as a clear oil (238 mg, 81%). ^{1}H NMR as previously reported.[26]

(S)-2-(tert-Butoxycarbonylamino)-L-phenylalaninol-1-^{13}C (17). To a solution of L-phenylalanine-1-^{13}C (100 mg, 0.6 mmol) in THF/methanol (1:6, 50 mL) were added triethylamine (125 mg, 1.2 mmol) and Boc$_2$O (147 mg, 0.65 mmol). The mixture was stirred at room temperature for 18 h. The mixture was acidified with 1 M HCl (25 mL). The solvent was removed *in vacuo*. The pale yellow oil was partitioned between EtOAc (50 mL) and H$_2$O (50 mL). The aqueous phase was extracted with EtOAc (2 × 50 mL). The combined organic phase was washed with H$_2$O (50 mL) and brine (50 mL) and dried over Na$_2$SO$_4$. The solvent was removed in vacuo to give a clear oil (190 mg), which was dissolved in anhydrous THF (25 mL) and cooled in an ice bath. LiAlH$_4$ (90 mg, 2.5 mmol) was suspended in anhydrous THF (5 mL) and added to the reaction mixture dropwise under Ar. The mixture was allowed to warm up to room temperature and stirred under N$_2$ for 18 h. H$_2$O (2 mL) was added dropwise to the ice-cooled reaction mixture. The volatiles were removed *in vacuo*. The aqueous solution was acidified with 2 M HCl (20 mL) and extracted with EtOAc (4 × 20 mL). The combined organic phase was washed with brine (2 × 20 mL) and dried over MgSO$_4$. The solvent was removed *in vacuo* to give compound **17** as a white solid (166 mg, quant). ^{1}H NMR (300 MHz, CDCl$_3$) δ 7.39 – 7.09 (m, 5H), 4.79 (br s, 1H), 4.05 – 3.82 (m, 2H), 3.75 – 3.47 (m, 1H), 2.87-2.81 (m, 2H), 1.42 (s, 9H). Analytical RP-HPLC: t_R = 17.1

min (A/B 100 : 0 to 0 : 100 in 20 min, λ = 220 nm). HRMS (ESI) found [M+Na]$^+$ 275.1458, C$_{13}$^{13}CH$_{21}$NNaO$_3$$^+$ requires 275.1453.

^{13}C-labelled macrocyclic alcohol **19.** Compound **17** (48 mg, 0.19 mmol) was dissolved in DCM (1 mL) and cooled in an ice bath. TFA (1 mL) was added slowly. The mixture was stirred for 1 h in an ice bath and the volatiles were removed *in vacuo* to give compound **18** as a clear oil, which was used in subsequent synthesis without further purification. Compound **14** (76 mg, 0.16 mmol) was dissolved in anhydrous DMF (1 mL). Compound **18** (27.6 mg, 0.18 mmol), HATU (68 mg, 0.18 mmol), HOBt (33 mg, 0.22 mmol) and DIPEA (93 mg, 0.72 mmol) were added. The mixture was stirred under N$_2$ at room temperature for 21 h before acidified to pH 1 with 1 M HCl. The mixture was diluted with EtOAc (20 mL). The organic phase was washed with 1 M HCl (16 mL), sat. NaHCO$_3$ (2 × 30 mL), H$_2$O (2 × 30 mL) and brine (40 mL) and dried over Na$_2$SO$_4$. The solvent was removed *in vacuo* and the resultant crude product was purified by flash chromatography (petroleum ether:EtOAc 1:4) to give compound **17** as a white solid (38 mg, 39%). ^{1}H NMR (600 MHz, CDCl$_3$) δ 10.95 (br s, 1H), 8.01 (br s, 1H), 7.23 – 7.07 (m, 5H), 6.99 (d, J = 8.1 Hz, 2H), 6.94 (d, J = 8.1 Hz, 2H), 6.73 (d, J = 8.1 Hz, 2H), 6.68 (d, J = 8.1 Hz, 2H), 6.20 (br s, 1H), 6.15 (br s, 1H), 5.29 – 5.19 (m, 1H), 4.30 – 4.21 (m, 1H), 4.04 – 3.87 (m, 5H), 3.77 – 3.60 (m, 2H), 3.38 (dd, J = 14.2, 5.7 Hz, 1H), 3.27 – 3.16 (m, 1H), 3.07 – 2.93 (m, 3H), 2.88 – 2.81 (m, 2H), 2.77 – 2.70 (m, 1H), 2.02 – 1.88 (m, 4H). Analytical RP-HPLC: t_R = 18.6 min (A/B 100 : 0 to 0 : 100 in 20 min, λ = 220 nm). HRMS (ESI) found [M+Na]$^+$ 633.2769, C$_{35}$^{13}CH$_{39}$N$_3$NaO$_6$$^+$ requires 633.2765.

2. NMR experiments

Solution A was prepared by resuspending compound **8** (2.6 mM) in 7.5% DMSO-d_6 in D$_2$O (1.05 mL) and filtering to remove the insoluble residues. Solution B was prepared by dissolving α-chymotrypsin (2.6 mM) in 20% DMSO-d_6 in D$_2$O (1.05 mL). Solution C was prepared by resuspending compound **8** (2.6 mM) in 20% DMSO-d_6 in D$_2$O (1.05 mL) and filtering to remove the insoluble residues. Solution D was prepared by combining solutions C (350 μL) and B (350 μL) All solutions were placed in separate glass NMR tubes and incubated at room temperature for 1 h with occasional inversions. ^{1}H NMR and ^{13}C NMR were collected for each solution using a Varian Inova 600 MHz instrument. The NMR spectra were processed by VnmrJ 3.2A.

3. Determining the Concentration of a saturated solution of 8 in DMSO/H$_2$O by RP-HPLC

Solutions of **8** in DMSO (100 μL, concentration = 0.2, 0.3, 0.4, 1, 1.5 and 2 mM) were prepared and 20 μL of each solution was subjected to RP-HPLC using an HP 1100 LC system equipped with a Phenomenex C-18 column (250 × 4.6 mm) with detection at λ = 280 nm. The absolute integral of the major peak at 18.1 min was calculated for each sample. The integrals were plotted against the calculated amount of **8** injected to construct a standard curve, as shown in Fig. 4. An excess amount of **8** was resuspended in 7.5% DMSO in H$_2$O with stirring at room temperature for 1 h. The sample was centrifuged and filtered to give a homogeneous solution and 20 μL of this solution was analysed by RP-HPLC. The absolute intergral of the peak at 18.1 min was matched with the standard curve to identify a concentration of 0.69 mM. Similarly, the concentration of a saturated solution of **8** in 20% DMSO in H$_2$O was determined to be 2.6 mM.

4. *In vitro* α-Chymotrypsin Assay

The activity of α-chymotrypsin was assayed spectrophotometrically at 25 ºC using Synergy H4 Hybrid Multi-Mode Microplate Reader. A solution of α-chymotrypsin (21.9 µg/mL) in 1 mM aqueous HCl was prepared freshly by a 1:40 dilution of a stock solution (874 µg/mL) in 1 mM aqueous HCl and kept on ice. A 1:100 dilution of the 21.9 µg/mL solution in ice-cold 1 mM aqueous HCl was prepared immediately before the start of each measurement. The assay was conducted in black 96-well plates as below: To each well was added AAF-AMC (Sigma Aldrich, Castle Hill, NSW) substrate in DMSO (5 µL, final concentrations = 0.5 mM), α-chymotrypsin in 1 mM aqueous HCl (10 µL, final concentration = 4 nM), DMSO (0, 15 or 35 µL) and Mili-Q water (185, 160, or 150 µL). The total volume in each well was 200 µL. The excitation and emission wavelengths are 380 nm and 460 nm respectively. Progress curves were monitored over 10 min. The assay was conducted in triplicate.

Acknowledgements

References

1. P. Madala, J. D. A. Tyndall, T. Nall and D. P. Fairlie, *Chem. Rev.*, 2010, **110**, PR1-31.
2. J. Phan, A. Zdanov, A. G. Evdokimov, J. E. Tropea, H. K. Peters, R. B. Kapust, M. Li, A. Wlodawer and D. S. Waugh, *J. Biol. Chem.*, 2002, **277**, 50564-50572.
3. X. Xue, H. Yu, H. Yang, F. Xue, Z. Wu, W. Shen, J. Li, Z. Zhou, Y. Ding, Q. Zhao, X. C. Zhang, M. Liao, M. Bartlam and Z. Rao, *J. Virol.*, 2008, **82**, 2515-2527.
4. M. Prabu-Jeyabalan, E. Nalivaika and C. A. Schiffer, *Structure*, 2002, **10**, 369-381.
5. L. Wu, L. Wang, G. Hua, K. Liu, X. Yang, Y. Zhai, M. Bartlam, F. Sun and Z. Fan, *J. Immunol.*, 2009, **183**, 421-429.
6. J. M. Wells and S. Strickland, *Development*, 1994, **120**, 3639-3647.
7. W. M. Kazmierski, R. L. Jarvest, J. J. Plattner and X. Li, in *Macrocycles in Drug Discovery*, The Royal Society of Chemistry, 2015, ch. 7, 235-282.
8. E. Marsault and M. L. Peterson, *J. Med. Chem.*, 2011, **54**, 1961-2004.
9. J. D. A. Tyndall, L. K. Pattenden, R. C. Reid, S.-H. Hu, D. Alewood, P. F. Alewood, T. Walsh, D. P. Fairlie and J. L. Martin, *Biochemistry*, 2008, **47**, 3736-3744.
10. J. D. A. Tyndall, R. C. Reid, D. P. Tyssen, D. K. Jardine, B. Todd, M. Passmore, D. R. March, L. K. Pattenden, D. A. Bergman, D. Alewood, S.-H. Hu, P. F. Alewood, C. J. Birch, J. L. Martin and D. P. Fairlie, *J. Med. Chem.*, 2000, **43**, 3495-3504.
11. S. Zaman, P. Campaner and A. D. Abell, *Biorg. Med. Chem.*, 2006, **14**, 8323-8331.
12. (a) A. Pehere and A. Abell, in *Proteases in Health and Disease*, eds. S. Chakraborti and N. S. Dhalla, Springer New York, 2013, vol. 7, ch. 11, pp. 181-192. (b) M. K. Edmonds and A. D. Abell, *J. Org. Chem.*, **2001**, *66*, 3747-3752.
13. S. A. Jones, S. Duncan, S. G. Aitken, J. M. Coxon and A. D. Abell, *Aust. J. Chem.*, 2014, **67**, 1257-1263.
14. Y. S. Tsantrizos, G. Bolger, P. Bonneau, D. R. Cameron, N. Goudreau, G. Kukolj, S. R. LaPlante, M. Llinàs-Brunet, H. Nar and D. Lamarre, *Angew. Chem. Int. Ed.*, 2003, **42**, 1356-1360.
15. S. Hanessian, G. Yang, J.-M. Rondeau, U. Neumann, C. Betschart and M. Tintelnot-Blomley, *J. Med. Chem.*, 2006, **49**, 4544-4567.
16. A. D. Pehere and A. D. Abell, *Org. Lett.*, 2012, **14**, 1330-1333.
17. D. L. Wilson, I. Meininger, Z. Strater, S. Steiner, F. Tomlin, J. Wu, H. Jamali, D. Krappmann and M. G. Götz, *ACS Med. Chem. Lett.*, 2016, **7**, 250-255.
18. N. J. Liverton, M. K. Holloway, J. A. McCauley, M. T. Rudd, J. W. Butcher, S. S. Carroll, J. DiMuzio, C. Fandozzi, K. F. Gilbert, S.-S. Mao, C. J. McIntyre, K. T. Nguyen, J. J. Romano, M. Stahlhut, B.-L. Wan, D. B. Olsen and J. P. Vacca, *J. Am. Chem. Soc.*, 2008, **130**, 4607-4609.
19. R. C. Reid, L. K. Pattenden, J. D. A. Tyndall, J. L. Martin, T. Walsh and D. P. Fairlie, *J. Med. Chem.*, 2004, **47**, 1641-1651.
20. D. Lamarre, P. C. Anderson, M. Bailey, P. Beaulieu, G. Bolger, P. Bonneau, M. Bos, D. R. Cameron, M. Cartier, M. G. Cordingley, A.-M. Faucher, N. Goudreau, S. H. Kawai, G. Kukolj, L. Lagace, S. R. LaPlante, H. Narjes, M.-A. Poupart, J. Rancourt, R. E. Sentjens, R. St George, B. Simoneau, G. Steinmann, D. Thibeault, Y. S. Tsantrizos, S. M. Weldon, C.-L. Yong and M. Llinas-Brunet, *Nature*, 2003, **426**, 186-189.
21. J. Zheng, C. Liu, M. R. Sawaya, B. Vadla, S. Khan, R. J. Woods, D. Eisenberg, W. J. Goux and J. S. Nowick, *J. Am. Chem. Soc.*, 2011, **133**, 3144-3157.
22. A. D. Abell, M. A. Jones, J. M. Coxon, J. D. Morton, S. G. Aitken, S. B. McNabb, H. Y. Y. Lee, J. M. Mehrtens, N. A. Alexander, B. G. Stuart, A. T. Neffe and R. Bickerstaffe, *Angew. Chem., Int. Ed.*, 2009, **48**, 1455-1458.
23. P. M. Neilsen, A. D. Pehere, K. I. Pishas, D. F. Callen and A. D. Abell, *ACS Chem. Biol.*, 2012, **8**, 353-359.
24. A. D. Pehere, M. Pietsch, M. Gütschow, P. M. Neilsen, D. S. Pedersen, S. Nguyen, O. Zvarec, M. J. Sykes, D. F. Callen and A. D. Abell, *Chem. Eur. J.*, 2013, **19**, 7975-7981.
25. D. R. March, G. Abbenante, D. A. Bergman, R. I. Brinkworth, W. Wickramasinghe, J. Begun, J. L. Martin and D. P. Fairlie, *J. Am. Chem. Soc.*, 1996, **118**, 3375-3379.
26. K. C. H. Chua, M. Pietsch, X. Zhang, S. Hautmann, H. Y. Chan, J. B. Bruning, M. Gütschow and A. D. Abell, *Angew. Chem. Int. Ed.*, 2014, **53**, 7828-7831.
27. L. Zhu, S. George, M. F. Schmidt, S. I. Al-Gharabli, J. Rademann and R. Hilgenfeld, *Antivir. Res.*, 2011, **92**, 204-212.
28. B. J. Votta, M. A. Levy, A. Badger, J. Bradbeer, R. A. Dodds, I. E. James, S. Thompson, M. J. Bossard, T. Carr, J. R. Connor, T. A. Tomaszek, L. Szewczuk, F. H. Drake, D. F. Veber and M. Gowen, *J. Bone Miner. Res.*, 1997, **12**, 1396-1406.
29. C. Ma, X. Li, X. liang, K. Jin, J. Cao and W. Xu, *Bioorg. Med. Chem. Lett.*, 2013, **23**, 4948-4952.
30. A. J. Harvey and A. D. Abell, *Bioorg. Med. Chem. Lett.*, 2001, **11**, 2441-2444.
31. Y. D. Ward, D. S. Thomson, L. L. Frye, C. L. Cywin, T. Morwick, M. J. Emmanuel, R. e. Zindell, D. McNeil, Y. Bekkali, M. Hrapchak, M. DeTuri, K. Crane, D. White, S. Pav, Y. Wang, M.-H. Hao, C. A. Grygon, M. E. Labadia, D. M. Freeman, W. Davidson, J. L. Hopkins, M. L. Brown and D. M. Spero, *J. Med. Chem.*, 2002, **45**, 5471-5482.
32. N. Asaad, P. A. Bethel, M. D. Coulson, J. E. Dawson, S. J. Ford, S. Gerhardt, M. Grist, G. A. Hamlin, M. J. James, E. V. Jones, G. I. Karoutchi, P. W. Kenny, A. D. Morley, K. Oldham, N. Rankine, D. Ryan, S. L. Wells, L. Wood, M. Augustin, S. Krapp, H. Simader and S. Steinbacher, *Bioorg. Med. Chem. Lett.*, 2009, **19**, 4280-4283.
33. S. D. Demo, C. J. Kirk, M. A. Aujay, T. J. Buchholz, M. Dajee, M. N. Ho, J. Jiang, G. J. Laidig, E. R. Lewis, F. Parlati, K. D. Shenk, M. S. Smyth, C. M. Sun, M. K. Vallone, T. M. Woo, C. J. Molineaux and M. K. Bennett, *Cancer Res.*, 2007, **67**, 6383-6391.
34. J. Zhang, M. Han, X. Ma, L. Xu, J. Cao, Y. Zhou, J. Li, T. Liu and Y. Hu, *Chem. Biol. Drug Des.*, 2014, **84**, 497-504.
35. F. Wångsell, K. Gustafsson, I. Kvarnström, N. Borkakoti, M. Edlund, K. Jansson, J. Lindberg, A. Hallberg, Å. Rosenquist and B. Samuelsson, *Eur. J. Med. Chem.*, 2010, **45**, 870-882.
36. S. D. Young, L. S. Payne, W. J. Thompson, N. Gaffin, T. A. Lyle, S. F. Britcher, S. L. Graham, T. H. Schultz and A. A. Deana, *J. Med. Chem.*, 1992, **35**, 1702-1709.
37. J. Adams, M. Behnke, S. Chen, A. A. Cruickshank, L. R. Dick, L. Grenier, J. M. Klunder, Y.-T. Ma, L. Plamondon and R. L. Stein, *Bioorg. Med. Chem. Lett.*, 1998, **8**, 333-338.
38. D. Pearson and A. D. Abell, *Org. Biomol. Chem.*, 2006, **4**, 3618-3625.
39. I. Schechter and A. Berger, *Biochem. Biophys. Res. Commun.*, 1967, **27**, 157-162.
40. W. C. Groutas, M. A. Stanga and M. J. Brubaker, *J. Am. Chem. Soc.*, 1989, **111**, 1931-1932.
41. J. A. Cleary, W. Doherty, P. Evans and J. P. G. Malthouse, *BBA - Proteins Proteom.*, 2014, **1844**, 1119-1127.
42. D. Neidhart, Y. Wei, C. Cassidy, J. Lin, W. W. Cleland and P. A. Frey, *Biochemistry*, 2001, **40**, 2439-2447.
43. D. O. Shah, K. Lai and D. G. Gorenstein, *J. Am. Chem. Soc.*, 1984, **106**, 4272-4273.
44. E. A. Clark, N. Walker, D. C. Ford, I. A. Cooper, P. C. F. Oyston and K. R. Acharya, *J. Biol. Chem.*, 2011, **286**, 24015-24022.
45. H. Kim, T. T. T. Chu, D. Y. Kim, D. R. Kim, C. M. T. Nguyen, J. Choi, J.-R. Lee, M.-J. Hahn and K. K. Kim, *J. Mol. Biol.*, 2008, **376**, 184-192.
46. A. Roussel, M. Mathieu, A. Dobbs, B. Luu, C. Cambillau and C. Kellenberger, *J. Biol. Chem.*, 2001, **276**, 38893-38898.

Organic & Biomolecular Chemistry Accepted Manuscript

Graphical Abstract
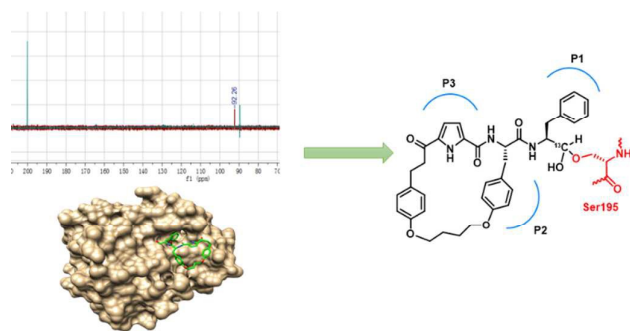
NMR and X-ray crystallography reveals covalent attachment of the macrocyclic aldehyde to serine195 of α-chymotrypsin and that its backbone binds as a β-strand.